IEEE Access
Multidisciplinary | Rapid Review | Open Access Journal

Received November 11, 2019, accepted December 5, 2019, date of publication December 10, 2019,
date of current version December 23, 2019.

Digital Object Identifier 10.1109/ACCESS.2019.2958739

A Low Complexity 16 × 16 Butler Matrix Design Using Eight-Port Hybrids

QINGLING YANG[1], STEVEN GAO[1], (Fellow, IEEE), QI LUO[1], (Senior Member, IEEE), LEHU WEN[1], XIAOFEI REN[2], JIAN WU[2], YONG-LING BAN[3], AND XUEXIA YANG[4], (Senior Member, IEEE)

[1]School of Engineering and Digital Arts, University of Kent, Canterbury CT2 7NZ, U.K.
[2]China Research Institute of Radiowave Propagation, Xinxiang 453003, China
[3]School of Electronic Science and Engineering, University of Electronic Science and Technology of China, Chengdu 611731, China
[4]School of Communication and Information Engineering, Shanghai University, Shanghai 200444, China

Corresponding author: Qingling Yang (qy31@kent.ac.uk)

This work was supported in part by the China Research Institute of Radiowave Propagation, Engineering and Physical Sciences Research Council (EPSRC) under Grant EP/P015840/1, Grant EP/S005625/1, and Grant EP/N032497/1, and in part by the Natural Science Foundation of China (NSFC) under Grant 61771300.

ABSTRACT Beamforming networks such as Butler Matrices are important for multibeam array antenna applications. The challenge for Butler Matrix design is that their complexity increases with the number of ports. In this paper, a novel approach of designing a 16 × 16 Butler Matrix with significant structure simplification is presented. The eight-port hybrids with no crossovers are used to simplify the network. To ensure the network has the same magnitude and phase responses as the standard one, the location and phase shifting value of each fixed phase shifter are derived from the S-matrix of each hybrid. A 16 × 16 Butler Matrix network operating from 9 GHz–11 GHz is designed to validate this concept. The compensated microstrip 3-dB/90° directional coupler, the phase shifter with a shunt open-and-short stub and the crossover with a resonating patch are used to reduce the transmission loss and enable broadband operation.

INDEX TERMS Butler matrix, directional coupler, eight-port hybrid, multibeam, phase shifter.

I. INTRODUCTION

In recent years, Butler Matrices have been widely used in microwave and millimeter-wave applications such as tracking [1], QAM multiport modulators [2] and multi-port amplifiers [3], etc. They offer the possibility of having multiple passive T/R channels and providing a good compromise between performance and cost [4]–[8]. Recent studies show that Butler Matrices can also be used to generate waves carrying orbital angular momentum (OAM) [9], [10].

In most cases, the 4 × 4 and 8 × 8 Butler Matrices are used because the complexity of these networks is relatively low [11]–[17]. As shown in Fig. 1, a standard 16 × 16 Butler Matrix [18] includes three different types of components, namely 3-dB/90° directional couplers, phase shifters and crossovers. In this figure, #1–#16 are beam ports and A_1–A_{16} are array ports. The circled $n\times$ represents a fixed phase shifter in multiples of $p = 180°n/N$, where $N = 16$ in this case. From Fig. 1, it is derived that for different beam port excitations the phase response at each array port varies as shown in Table 1, where i is the sequence number of array port A_i. In this standard Butler Matrix, the total number

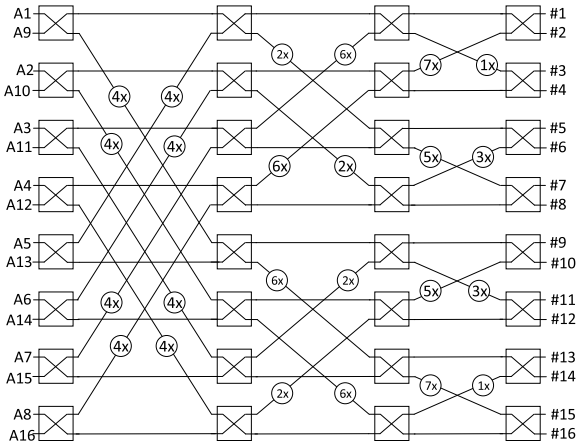

FIGURE 1. Schematic diagram of a standard 16 × 16 Butler Matrix. The circled n× represents fixed phase shifter in multiples of p = 180°n/N, i.e. p = 11.25°n. #1–#16 are beam ports, and A_1–A_{16} are array ports.

The associate editor coordinating the review of this manuscript and approving it for publication was Feng Lin.

TABLE 1. Phase response in a standard 16 × 16 Butler Matrix.

Feed	Output Phase	Feed	Output Phase
#1	$-p(i-1)$	#2	$-8p+15p(i-1)$
#3	$-7p-9p(i-1)$	#4	$-15p+7p(i-1)$
#5	$-6p-5p(i-1)$	#6	$14p+11p(i-1)$
#7	$-9p-13p(i-1)$	#8	$15p+3p(i-1)$
#9	$-4p-3p(i-1)$	#10	$-12p+13p(i-1)$
#11	$-9p-11p(i-1)$	#12	$15p+5p(i-1)$
#13	$-6p-7p(i-1)$	#14	$-14p+9p(i-1)$
#15	$-7p-15p(i-1)$	#16	$-15p+p(i-1)$

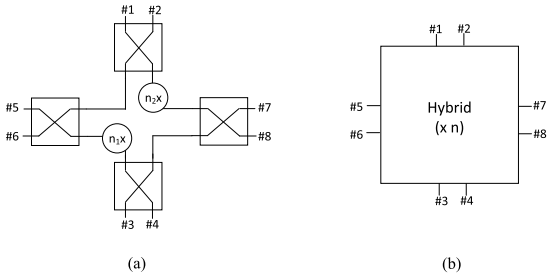

FIGURE 2. Eight-port hybrid. (a) Topology. (b) Footprint of the eight-port hybrid.

of these components is 116 (which includes 32 3-dB/90° directional couplers, 24 phase shifters and 60 crossovers). Notably, the percentage of the crossovers in this network is higher than 50%. The extremely high complexity make it very difficulty to design and fabricate a 16 × 16 Butler Matrix.

In this paper, a novel approach to design an equivalent 16 × 16 Butler Matrix is presented. The network is designed based on an eight-port hybrid, which has been reported as the comparator in monopulse antennas or four-way power dividers and combiners [19]–[21]. The structure of an eight-port hybrid consists of four 3-dB/90° directional couplers and two fixed phase shifters, and no crossings are needed. In this proposed network, eight this type of hybrids are required. Hence, the complexity of the proposed network can be greatly reduced with only four crossovers. Detailed synthesis procedures are developed in Section II. To obtain the same transmission magnitude and phase responses as a standard 16 × 16 Butler Matrix, the location and phase shifting value of each fixed phase shifter are determined by the deviations based on the S-matrix of each hybrid.

For the ease of realization, Butler Matrices utilizing microstrip structures are preferred. However, one of disadvantages of a microstrip Butler Matrix is that the operating bandwidth is narrow. In this design, to achieve broadband operation, the microstrip-based compensated 3-dB/90° directional coupler is used. Compared with the multi-section branchline directional couplers, the compensated coupler can provide less transmission loss and lower output amplitude/phase imbalance over the operating bandwidth [22], [23]. The microstrip phase shifters are realized by taking a microstrip line shunt with an open- and short-stub as a reference. Compared with the multisection Schiffman phase shifters, the used phase shifters have broader bandwidth and larger phase shift range [24]. In addition, the operation bandwidth of the crossover is improved by the combination of a ring-shaped coupler and a radial resonating patch [25]. Thus, multiple resonances over the operating bandwidth are introduced. The proposed design of the 16 × 16 Butler Matrix has been experimentally validated with a prototype operating from 9 GHz to 11 GHz.

II. METHODOLOGY

Fig. 2 shows the topology of the eight-port network, which consists of four 3-dB/90° directional couplers and two fixed phase shifters. #1–#4 are the feeding ports and #5–#8 are output ports. For any feeding port excitation, the signals output from #5–#8 have the same magnitude but in different phase, and the rest of feeding ports are isolated. In this hybrid, all the directional couplers are oriented to different directions and no crossings are required. Hence, the complexity of the proposed network formed by this type of hybrids is significantly reduced compared with a standard 16 × 16 Butler Matrix. To make a network equivalent to a standard 16 × 16 Butler Matrix, the relationship between the two phase shifters in a hybrid is defined as follows [18], [20]:

$$p(n_1+n_2)=\pm 90^\circ \tag{1}$$

where $p = 11.25^\circ$, n_1 and n_2 are integers and are satisfied $n_1 n_2 > 0$. To facilitate the analysis, the eight-port hybrid is transformed into an equivalent module shown in Fig. 2(b). In this module, n equals n_1, and n_2 is substituted by using (1), namely

$$n_2=\pm\frac{90^\circ}{p}-n_1=\pm\frac{90^\circ}{p}-n \tag{2}$$

The relationship between excitations and responses are characterized by its S-matrix, which is expressed as:

$$[S]=\frac{1}{2}\begin{bmatrix} O & B^T \\ B & O \end{bmatrix} \tag{3}$$

where O is a null matrix and

$$B=\begin{bmatrix} -1 & j & -e^{-jnp} & je^{-jnp} \\ j & 1 & -je^{-jnp} & -e^{-jnp} \\ je^{jnp} & -e^{jnp} & 1 & j \\ e^{jnp} & je^{jnp} & j & -1 \end{bmatrix} \tag{4}$$

As shown in Fig. 3, the proposed network consists of eight hybrids. All the hybrids have the same structure and the only difference comes from their fixed phase shifters having different phase shifts. The eight hybrids include 24 3-dB/90° directional couplers and 16 phase shifters in total. To obtain the same phase responses as the standard 16 × 16 Butler Matrix, the rest of eight phase shifters are positioned outside the hybrids.

The required phase response at each output port is determined by the cascading S-matrices. From Fig. 3, one can

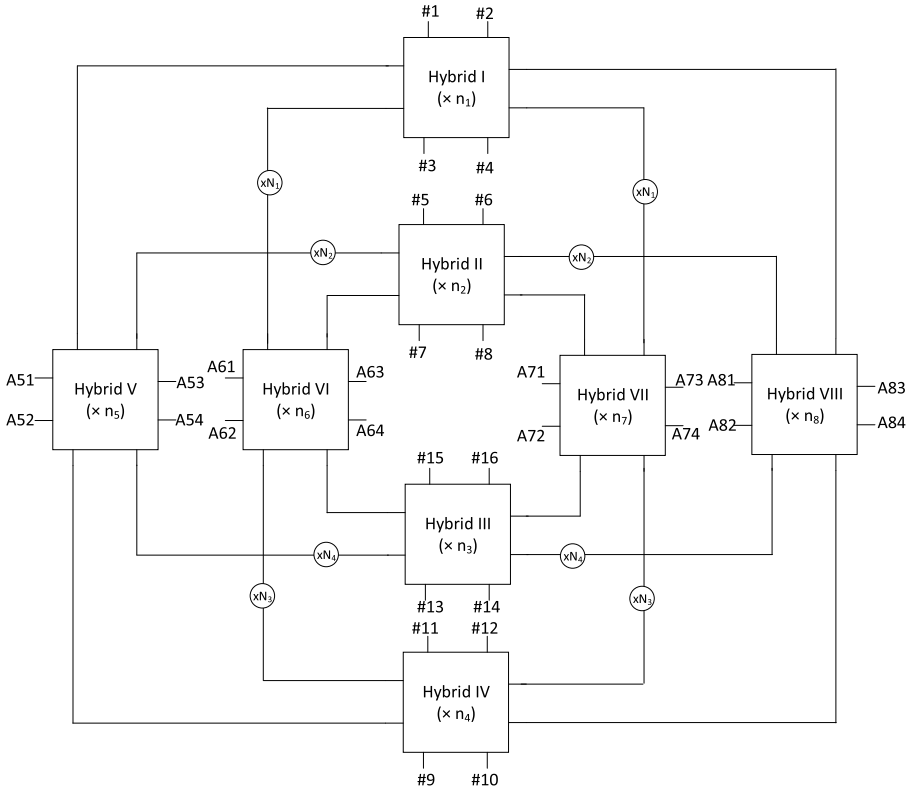

FIGURE 3. Proposed 16 × 16 Butler Matrix network composed of eight-port hybrids.

learn that for each signal flowing from a feeding port to each array port it should travel through two hybrids. Hence, the magnitude and phase responses of the full network can be obtained by their S-matrices from (3). The transmission magnitude and phase responses at the array ports of Hybrid V when port #1 is excited are obtained as follows:

$$[S_{A51,1}, S_{A52,1}, S_{A53,1}, S_{A54,1}] = \frac{1}{4}[1, -j, -je^{jn_5p}, -e^{jn_5p}] \tag{5}$$

where n_5 represents the fixed phase shifter in Hybrid V having phase shift of n_5p. With the same method, the phase responses at the array ports of Hybrid VI–VIII when the beam port #1 is excited can also be obtained. They are summarized as follows:

$$\begin{aligned}&[S_{A61,1}, S_{A62,1}, S_{A63,1}, S_{A64,1}]\\ &\quad = \frac{1}{4}[-je^{jN_1p}, -e^{jN_1p}, -e^{j(n_6+N_1)p}, je^{j(n_6+N_1)p}]\end{aligned} \tag{6}$$

$$\begin{aligned}&[S_{A71,1}, S_{A72,1}, S_{A73,1}, S_{A74,1}]\\ &\quad = \frac{1}{4}[je^{j(n_1+N_1)p}, e^{j(n_1+N_1)p},\\ &\qquad -e^{j(n_1+n_7+N_1)p}, je^{j(n_1+n_7+N_1)p}]\end{aligned} \tag{7}$$

$$\begin{aligned}&[S_{A81,1}, S_{A82,1}, S_{A83,1}, S_{A84,1}]\\ &\quad = \frac{1}{4}[-e^{jn_1p}, je^{jn_1p}, -je^{j(n_1+n_8)p}, -e^{j(n_1+n_8)p}]\end{aligned} \tag{8}$$

From Table 1, one can learn that for #1 excitation in a standard 16 × 16 Butler Matrix, the phase response at each array port is $-p(i-1)$ $(i = 1, 2, \ldots, 16)$, where i is the sequence number of the array port A_i. By comparing them with the derived phase values in (5)–(8), one can obtain that only when

$$\begin{aligned}&n_1 = 1, \quad n_5 = n_6 = 4,\\ &n_7 = n_8 = -4, \quad N_1 = 6\end{aligned} \tag{9}$$

(5)–(8) can be solved at the same time. In addition, it should be noted that the array ports of the hybrids and the array ports in Fig. 1 needs to satisfy the following equivalences:

$$\begin{aligned}&A_{51} \longleftrightarrow A_1, \quad A_{52} \longleftrightarrow A_9,\\ &A_{53} \longleftrightarrow A_5, \quad A_{54} \longleftrightarrow A_{13}\\ &A_{61} \longleftrightarrow A_3, \quad A_{62} \longleftrightarrow A_7,\\ &A_{63} \longleftrightarrow A_{11}, \quad A_{64} \longleftrightarrow A_{15}\\ &A_{71} \longleftrightarrow A_8, \quad A_{72} \longleftrightarrow A_{16},\\ &A_{73} \longleftrightarrow A_4, \quad A_{74} \longleftrightarrow A_{12}\\ &A_{81} \longleftrightarrow A_6, \quad A_{82} \longleftrightarrow A_{14},\\ &A_{83} \longleftrightarrow A_2, \quad A_{84} \longleftrightarrow A_{10}\end{aligned}$$

They indicate that in a standard 16 × 16 Butler Matrix the array ports $A_i, A_{i+4}, A_{i+8}, A_{i+12}$ $(i = 1, \ldots, 4)$ are included in the same eight-port hybrid. The obtained phase shifts in (9) are validated when port #2 – #4 is excited separately. Combining the phase responses in Table 1, the rest of unknowns of the network in Fig. 3 are worked out and validated with the same method according to the corresponding phase responses when

the feeding port from Hybrid II–IV is excited. The obtained values of these unknown parameters are

$$n_2 = 5, \quad n_3 = -1, \; n_4 = -5,$$
$$N_2 = N_3 = 2, \quad N_4 = 6 \tag{10}$$

By comparing the proposed network formed by eight-port hybrids with the standard 16 × 16 Butler Matrix, it is found that they have the same fixed phase shifters. The main difference is that these phase shifters are located in different places. Since these two networks are designed to have the same magnitude and phase responses, they can be considered as two equivalent networks but have different forms. Compared with the standard 16×16 Butler Matrix, the developed 16×16 Butler Matrix network has three significant advantages:

1) It has much lower complexity than the standard 16 × 16 Butler Matrix. In this designed network, only four crossovers are required and the whole structure is very symmetrical. This helps lower the design complexity and improve the design efficiency. All the crossovers are located outside the hybrids. Thus, the crossover design can be carried out independently without considering the phase shifters. In addition, one can select a transmission line as the reference path to design the phase shifters. In comparison, it takes the crossover as a reference path when designing phase shifters of a conventional Butler Matrix. Since the group delay or phase response of a crossover is quite different from the phase shifter, it is difficult to design a broadband phase shifter with a favourable phase shift.
2) All the hybrids share the same structure. Hence, the modular design with great flexibility can accelerate the overall design.
3) The network is designed in a smaller size and is realized on a single laminate with PCB processing technology.

III. REALIZATION OF THE PROPOSED NETWORK

Since the complexity of the network is greatly reduced, when comes to its physical realization, the biggest challenge is how to ensure its transmission performances including low loss, good amplitude and phase response. In this network, each input signal travels through seven essential components before flowing out from an array port, as shown in Fig. 4. However, it should be noted that the transmission loss and amplitude/phase errors from each component will be accumulated progressively. For instance, the errors from the directional couplers will be quadrupled at each array port since there are four directional couplers in the signal path. Hence, it is desirable that the 3-dB/90° directional couplers and phase shifters are operated with good amplitude and phase characteristics in a broadband.

The used structures of components are illustrated in Fig. 5. As shown in Fig. 5(a), the 3-dB/90° directional coupler is realized by connecting a series transmission line and a shunt open-stub with electrical lengths $\theta_1 = \theta_2 = 180°$ to each port of a ring-shaped 3-dB/90° directional coupler.

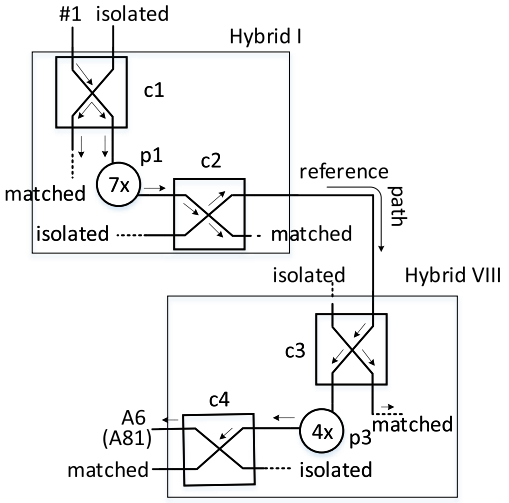

FIGURE 4. Signal path from the beam port #1 to array port A6 (or A81 for Hybrid VIII).

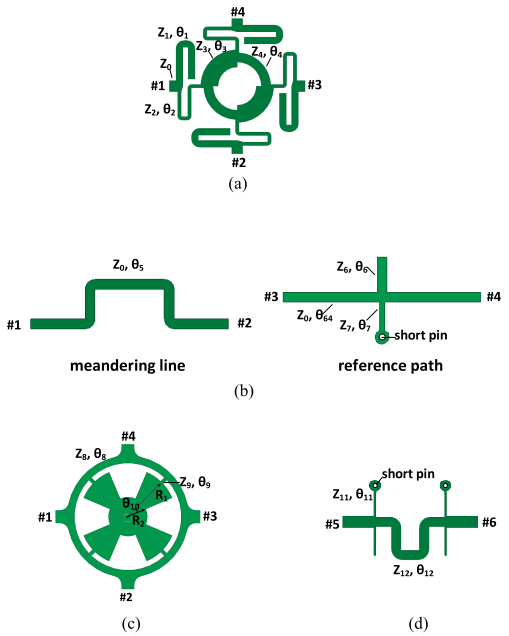

FIGURE 5. Component structures. (a) 3-dB/90° directional coupler. (b) Phase shifter and its reference path. (c) Crossover. (d) Reference path of the crossover.

The characteristic impedance of the $\lambda/2$ transmission line is 87Ω. For the shunt $\lambda/2$ open stub, this value is 65Ω. The series line and open stub are bended for the purpose of compactness. For this type of directional coupler, the performance at the center frequency is not affected by adding the $\lambda/2$ transmission line or branch. However, the impedance off the center frequency is compensated. As a result, the amplitude and phase variation of this 3-dB/90° directional coupler is only -3.15 ± 0.13 dB and $90.6 \pm 0.6°$ from 9 GHz to 11 GHz respectively while the return loss and port isolation are higher than 20 dB.

As to the phase shifter design shown in Fig.5(b), its reference path is formed with a microstrip line shunt with an

open and a short stub. To ensure the phase shifter operated over a broad bandwidth, the phase slope disparity between the microstrip line and reference path should be as small as possible. Since the reference path has a more dispersive phase response, the phase slope between them can be easily manipulated in a broad frequency range by varying (θ_6, Z_6) and (θ_7, Z_7). With the aid of a genetic algorithm (GA) code, a reference path for all the phase shifters are optimized, where $(\theta_6, Z_6) = (20°, 66\Omega)$ and $(\theta_7, Z_7) = (58°, 70\Omega)$. The obtained phase shifts for different phase shifters are in the range of $11.1° \pm 2.3°$, $22.9° \pm 1.3°$, $34.4° \pm 0.1°$, $44.3° \pm 1.1°$, $56° \pm 2.4°$, $67.3° \pm 0.9°$ and $78.7° \pm 1.5°$ over the operating bandwidth. In addition, the meandering path of the phase shifters connecting two submatrices is adjusted to meet the requirments of low transmission loss and compactness.

As shown in Fig. 5(c), the crossover is realized by combining a ring-shaped coupler with a radial resonating patch. The electrical lengths between two adjacent ports of this crossover are approximately $\lambda/2$. The radial resonating patch is designed to provide multi-resonances in the circular cavity. Hence, operation bandwidth of the designed crossover is enhanced accordingly. The simulated port isolation and return loss are higher than 16 dB over the operating bandwidth. The transmission loss at the center frequency 10 GHz is only 0.25 dB, and at 9 GHz and 11 GHz this value reaches 0.43 dB. In addition, as the group delay of this crossover is very different from that of a microstrip line, a broadband crossover reference path is introduced, as shown in Fig. 5(d). The simulated phase deviation between cross transmission of the designed crossover and the reference does not exceed $-0.3°$ to $0.9°$ over the operating bandwidth. Thus, it can be taken that the group delay from the crossover is canceled out and a flat phase response is achieved in the operating frequency range.

IV. EXPERIMENTAL RESULTS

Fig. 6 shows the fabricated prototype. It is realized on a RO4003C laminate having thickness of 0.508 mm, the relative dielectric constant $\varepsilon_r = 3.55$, and the loss tangent $\tan\delta = 0.0027$ at 10 GHz. The dimension of the fabricated 16 × 16 Butler Matrix network is 165 mm × 165 mm ($5.5\lambda_0 \times 5.5\lambda_0$). The simulated and measured reflection coefficients as well as the coupling between port #1 and all the remaining input ports are shown in Fig. 7 and Fig. 8, respectively. It can be seen that the return loss is higher than 10 dB from 9 GHz to 11 GHz and in the frequency range from 9.2 GHz–10.3 GHz the return loss is higher than 15 dB. The couplings between port 1 and all the other ports are less than –15 dB from 9.25 GHz to 10.5 GHz, and it is less than –10 dB in 9 GHz–11GHz. The measured results agree well with the simulated ones. Due to the structure symmetry, similar coupling levels are obtained from the remaining beam port measurement.

The transmission coefficient is one of another key parameters in determining the overall performance of the proposed 16 × 16 Butler Matrix network. As shown in Fig. 9 (a) and (b), the simulated coefficients at 10 GHz and

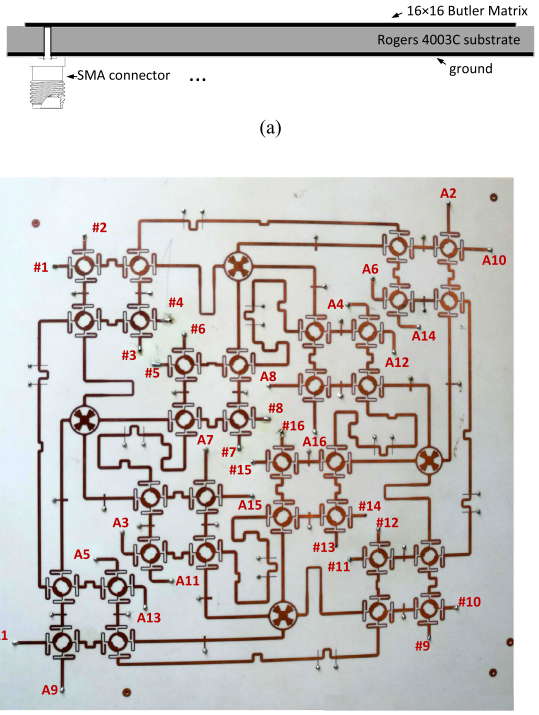

FIGURE 6. Fabricated prototype. (a) Side view of the designed 16 × 16 Butler Matrix network. (b) Fabricated prototype, where #*i* is the beam port and *Ai* is the array port(i = 1, . . ., 16).

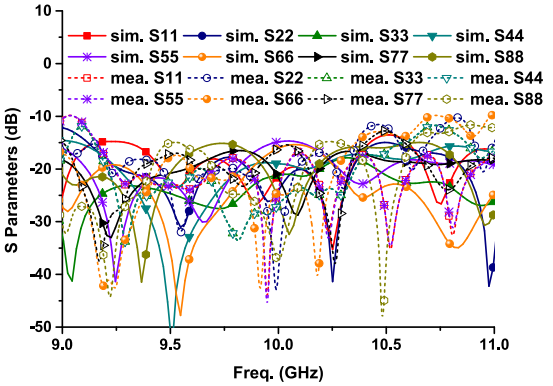

FIGURE 7. Simulated and measured reflection coefficients of port #1–#8.

9 GHz are -14 ± 0.6 dB and -14.5 ± 1.5 dB, while the measured ones are -14.5 ± 1 dB at 10 GHz and -15 ± 1 dB at 9 GHz. Considering that each signal from a beam port to any array port must travel through seven components and dispersion is progressively accumulated, the transmission coefficient fluctuations shown in Fig. 9 is in a relatively low level. The measured transmission coefficients are averagely 0.6 dB less than the simulated ones, as shown in Fig. 9 (c) and (d). The calculated dielectric loss for RO4003C laminate with thickness of 0.508 mm is approximately 0.006 dB/mm. The signal traveling length from a beam port to an array port is about 210 mm. Thus, it is estimated that the dielectric

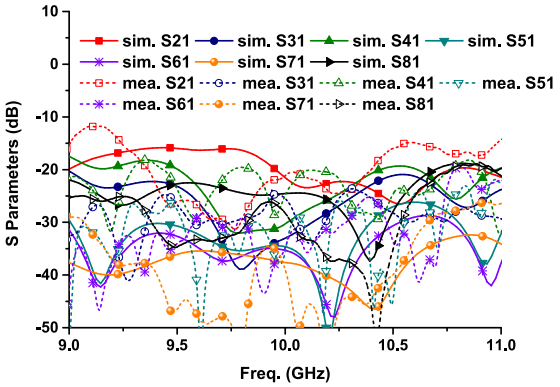

FIGURE 8. Simulated and measured coupling coefficients for port #1.

loss is 1.3 dB. In addition, since there are 16 beam ports in the designed network, the port mismatching and mutual couplings between the beam ports also contribute to some transmission loss. As can be seen from Fig. 7 and Fig. 8, the simulated port mismatching and mutual coupling are 0.043 dB on average for each port. Thus, the power dissipation caused by port mismatching and mutual couplings is about 0.7 dB in total. As a result, the total loss which includes dielectric loss, port mismatching and mutual coupling is about 2 dB.

The simulated and measured output phase differences between adjacent array ports are illustrated in Fig. 10. The simulated phase differences for beam port #1–# 8 excitation at 10 GHz are $11.5 \pm 8°$, $-168 \pm 8°$, $101 \pm 4°$, $-78.5 \pm 6.5°$, $57.4 \pm 3°$, $-123.9 \pm 3.2°$, $145 \pm 4°$, $-32.5 \pm 4.8°$, respectively. They are very close to the theoretical values. The phase differences at 9 GHz are slightly different to those at 10 GHz. This is because that errors caused by phase shifters are higher at edge frequencies than those at center frequency. At 9 GHz, the maximum phase deviation comes from beam port #2 excitation, which ranges in $-170.7 \pm 12.2°$. Due to the existence of RF connectors, fabrication and measurement errors, the dispersions of measured phase differences are higher than the simulated ones. For example, the measured phase differences at 10 GHz are $11.3 \pm 10.3°$, $-167.5 \pm 11.2°$, $102.8 \pm 8.2°$, $-79.7 \pm 9.4°$, $58.5 \pm 7.8°$, $-124.7 \pm 8.5°$, $147.4 \pm 6.7°$, $-31.2 \pm 7.6°$, while the measured maximum phase deviation at 9 GHz for beam port #2 is $-169.8 \pm 15.8°$.

The performance of the designed Butler Matrix in comparison with the results of other reported works [14], [26]–[28] are given in Table 2. Although the Butler Matrix shown in [28] also has the order of 16 × 16, a large number of crossovers are required and they are realized by external connections which result in poor performance and bulky size. The designed network has comparative performance when it compares with the 8×8 Butler Matrices reported in [14], [26], [27]. It has relatively low insertion loss, imbalance of transmission magnitudes and phase differences. The designed 16 × 16 Butler Matrix can be realized on a single laminate with low cost. In contrast, the reported Butler

TABLE 2. Comparison between the proposed 16 × 16 Butler Matrix and reported designs.

	[14]	[26]	[27]	[28]	This work
Order	8x8	8x8	8x8	16x16	16x16
f_0(GHz)	3	2.5	60	5	10
Size(mm^2)	170x145	n.a.	1.45x0.93	n.a.	165x165
BW(%)	33	16	17	3	20
Insertion Loss(dB)	1	1	3.1	4	2
Phase Variation(°)	±10	±6.2	±22	±24	±16
Amplitude Variation(dB)	±0.5	±1.76	±2.6	n.a.	±1.25
Realization Layer	difficult, stripline multiple	easy, microstrip single	difficult, CMOS multiple	difficult, microstrip multiple	easy, microstrip single

TABLE 3. Phase differences in x- and y-direction of the planar array, and calculated beam angles based on the measured *S*-parameters at 10 GHz. (unit: degree).

#1	#5	#9	#13
$\Phi_x = -4\times$, $\Phi_y = -1\times$, $\phi_0 = 13$, $\theta_0 = 12$.	$\Phi_x = 12\times$, $\Phi_y = -5\times$, $\phi_0 = 158$, $\theta_0 = 39$.	$\Phi_x = -12\times$, $\Phi_y = -3\times$, $\phi_0 = 14$, $\theta_0 = 37$.	$\Phi_x = 4\times$, $\Phi_y = -7\times$, $\phi_0 = 121$, $\theta_0 = 22$.
#2	#6	#10	#14
$\Phi_x = -4\times$, $\Phi_y = 15\times$, $\phi_0 = 286$, $\theta_0 = 49$	$\Phi_x = 12\times$, $\Phi_y = 11\times$, $\phi_0 = 221$, $\theta_0 = 53$.	$\Phi_x = -12\times$, $\Phi_y = 13\times$, $\phi_0 = 315$, $\theta_0 = 64$.	$\Phi_x = 4\times$, $\Phi_y = 9\times$, $\phi_0 = 244$, $\theta_0 = 28$.
#3	#7	#11	#15
$\Phi_x = -4\times$, $\Phi_y = -9\times$, $\phi_0 = 65$, $\theta_0 = 27$.	$\Phi_x = 12\times$, $\Phi_y = -13\times$, $\phi_0 = 134$, $\theta_0 = 65$.	$\Phi_x = -12\times$, $\Phi_y = -11\times$, $\phi_0 = 42$, $\theta_0 = 55$.	$\Phi_x = 4\times$, $\Phi_y = -15\times$, $\phi_0 = 106$, $\theta_0 = 50$.
#4	#8	#12	#16
$\Phi_x = -4\times$, $\Phi_y = 7\times$, $\phi_0 = 301$, $\theta_0 = 22$.	$\Phi_x = 12\times$, $\Phi_y = 3\times$, $\phi_0 = 193$, $\theta_0 = 37$.	$\Phi_x = -12\times$, $\Phi_y = 5\times$, $\phi_0 = 339$, $\theta_0 = 40$.	$\Phi_x = 4\times$, $\Phi_y = 1\times$, $\phi_0 = 192$, $\theta_0 = 11$.

Matrices shown in Table 2 need to be realized on multiple laminate layers and therefore have high complexity.

The designed 16 × 16 Butler Matrix can be used as the feeding network of a linear antenna array. The array factors are validated by applying the measured *S*-parameters, as shown in Fig. 11. Since the measured phase errors and amplitude imbalance at the edge frequencies are higher than those at the center frequency, the radiation patterns at the edge frequencies are degraded to a certain degree. These effects of the designed 16 × 16 Butler Matrix are caused by the inherent characteristics of microstrip lines, such as narrow bandwidth, very dispersive phase response and high insertion loss. At 9 GHz, the errors of beam pointing angles for different port excitations are increased to 14.8° and the side lobe levels are deteriorated to –5.4 dB. To minimize these side effects, striplines can be considered to realize the network as they have wide bandwidth, less dispersion and lower loss. The designed network can also be used to feed planar antenna arrays. The arrangement of array ports are illustrated in Fig. 12. As shown in Table. 3, the maximum

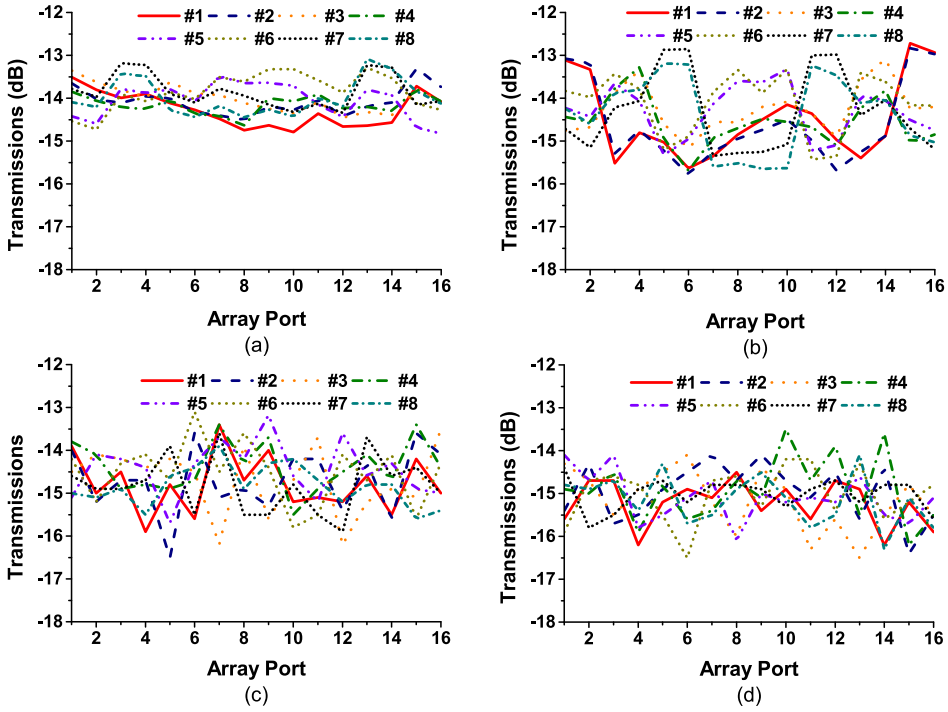

FIGURE 9. Simulated and measured transmission coefficients of the designed 16 × 16 Butler Matrix network. (a) Simulated at 10 GHz. (b) Simulated at 9 GHz. (c) Measured at 10 GHz. (d) Measured at 9 GHz.

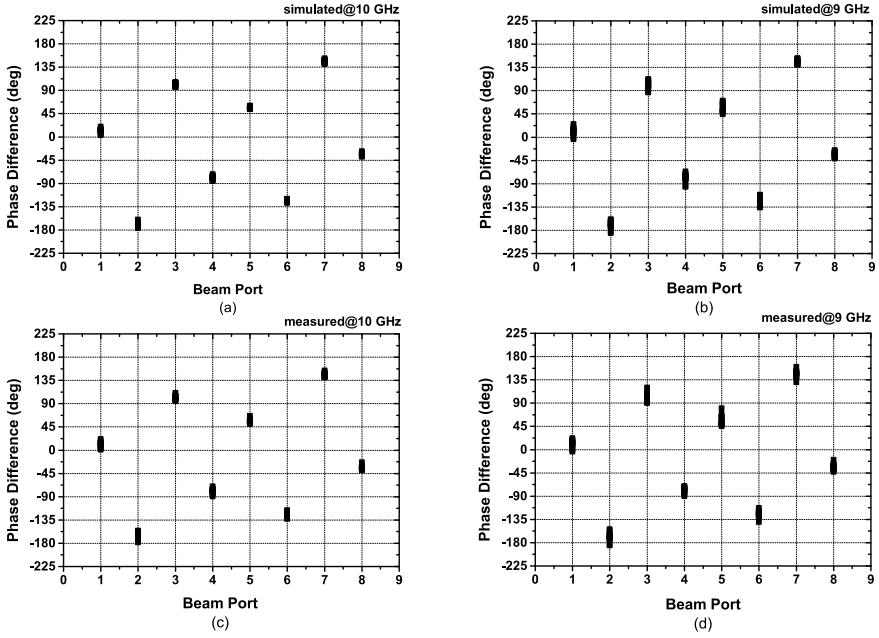

FIGURE 10. Simulated and measured output phase differences of the designed 16 × 16 Butler Matrix network. (a) Simulated at 10 GHz. (b) Simulated at 9 GHz. (c) Measured at 10 GHz. (d) Measured at 9 GHz.

phase difference in x- and y-direction is $12p$ and $-13p$, respectively. To ensure that all the beams are located in the real space and the grating lobes are in the imaginary space, the element spacing in x- and y-direction should be greater than $0.55\lambda_0$ and less than $0.7\lambda_0$ [29]. Therefore the element spacing in x- and y-direction are selected to be $d_x = d_y = 0.6\lambda_0$. Fig. 13 shows the radiation contours of the planar array calculated with the use of the measured S-parameters of the designed Butler Matrix. The beam angles for different beam port excitations are listed in Table. 3. The spatial radiation

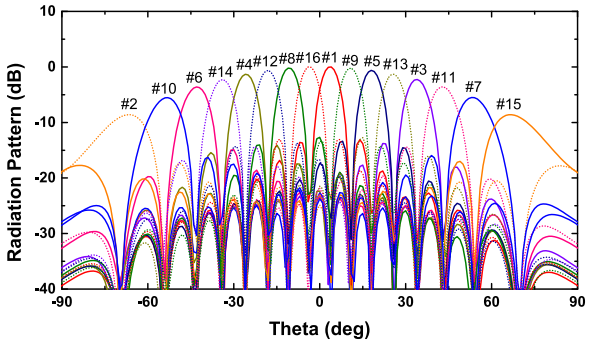

FIGURE 11. Radiation pattern of a linear antenna array fed by the designed 16 × 16 Butler Matrix network at 10 GHz.

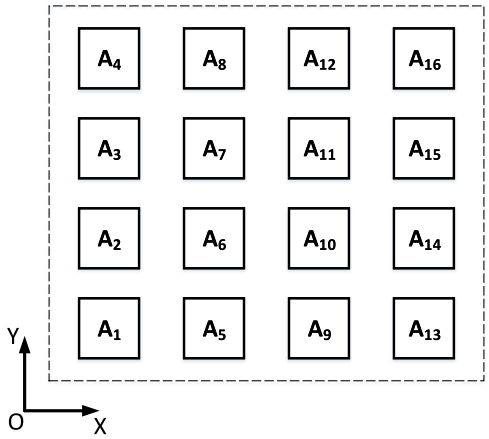

FIGURE 12. Element arrangement of 4×4 a planar array fed by the 16 × 16 Butler Matrix.

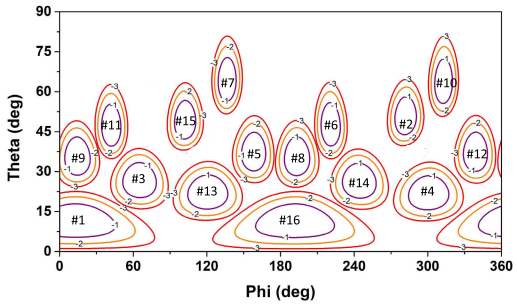

FIGURE 13. 2D radiation patterns of the planar array fed by the designed 16 × 16 Butler Matrix network at 10 GHz.

coverage, which is defined by the –3 dB beam contours, occupies approximately 60% of the half space.

V. CONCLUSION

A novel approach to design a 16 × 16 Butler Matrix network with simple configuration and broadband operation has been presented. The proposed design is based on the eight-port hybrids. The number of components in the proposed structure is reduced significantly, from 116 to 60, where the number of crossovers is only four. The proposed 16 × 16 Butler Matrix network can be realized on a single laminate. In this design, good transmission and phase characteristics are ensured by using the compensated 3-dB/90° directional couplers, the phase shifters with an open- and a short-stub, and the crossovers with a resonating patch. This proposed 16 × 16 Butler Matrix network can be applied in the linear or planar multibeam antenna arrays to realize 1D or 2D beam switching.

REFERENCES

[1] N. V. Priyadarshan and A. Thenmozhi, "Beam forming network using 4×4 narrowband Butler matrix for tracking and localization applications," in *Proc. Int. Conf. Intell. Comput. Control Syst. (ICICCS)*, Madurai, India, 2017, pp. 1241–1246.

[2] K. Staszek, S. Gruszczynski, and K. Wincza, "Direct N-QAM multiport modulators utilizing Butler matrices," in *Proc. 21st Int. Conf. Microw., Radar Wireless Commun. (MIKON)*, Kraków, Poland, 2016, pp. 1–4.

[3] A. Angelucci, P. Audagnotto, P. Corda, and B. Piovano, "Multiport power amplifiers for mobile-radio systems using microstrip Butler matrices," in *Proc. IEEE Antennas Propag. Soc. Int. Symp. URSI Nat. Radio Sci. Meeting*, Seattle, WA, USA, Jun. 1994, pp. 628–631.

[4] W. Hong, Z. H. Jiang, C. Yu, J. Zhou, P. Chen, Z. Yu, H. Zhang, B. Yang, X. Pang, M. Jiang, Y. Cheng, M. K. Taher Al-Nuaimi, Y. Zhang, J. Chen, and S. He, "Multibeam antenna technologies for 5G wireless communications," *IEEE Trans. Antennas Propag.*, vol. 65, no. 12, pp. 6231–6249, Dec. 2017.

[5] Y. C. Tsai, Y. B. Chen, and R. B. Hwang, "Combining the switched-beam and beam-steering capabilities in a 2-D phased array antenna system," *Radio Sci.*, vol. 51, pp. 47–58, Jan. 2016.

[6] Q.-L. Yang, Y.-L. Ban, K. Kang, C.-Y.-D. Sim, and G. Wu, "SIW multibeam array for 5G mobile devices," *IEEE Access*, vol. 4, pp. 2788–2796, 2016.

[7] A. Bhattacharyya, *Phased Array Antennas: Floquet Analysis, Synthesis, BFNs and Active Array Systems*. New York, NY, USA: Wiley, 2006.

[8] Y. Li, J. Wang, and K.-M. Luk, "Millimeter-wave multibeam aperture-coupled magnetoelectric dipole array with planar substrate integrated beamforming network for 5G applications," *IEEE Trans. Antennas Propag.*, vol. 65, no. 12, pp. 6422–6431, Dec. 2017.

[9] K. Murata, N. Honma, K. Nishimori, N. Michishita, and H. Morishita, "Analog eigenmode transmission for short-range MIMO based on orbital angular momentum," *IEEE Trans. Antennas Propag.*, vol. 65, no. 12, pp. 6687–6702, Dec. 2017.

[10] B. Palacin, K. Sharshavina, K. Nguyen, and N. Capet, "An 8×8 Butler matrix for generation of waves carrying orbital angular momentum (OAM)," in *Proc. 8th Eur. Conf. Antennas Propag. (EuCAP)*, The Hague, The Netherlands, 2014, pp. 2814–2818.

[11] S. Gruszczynski and K. Wincza, "Broadband 4×4 Butler matrices as a connection of symmetrical multisection coupled-line 3-dB directional couplers and phase correction networks," *IEEE Trans. Microw. Theory Techn.*, vol. 57, no. 1, pp. 1–9, Jan. 2009.

[12] J. K. Lee and K. Chang, "Dual-band switched beam array fed by dual-band Butler matrix," *Electron. Lett.*, vol. 47, no. 21, pp. 1164–1165, Oct. 2011.

[13] G. Tian, J.-P. Yang, and W. Wu, "A novel compact Butler matrix without phase shifter," *IEEE Microw. Wireless Compon. Lett.*, vol. 24, no. 5, pp. 306–308, May 2014.

[14] K. Wincza and S. Gruszczynski, "Broadband integrated 8×8 Butler matrix utilizing quadrature couplers and Schiffman phase shifters for multibeam antennas with broadside beam," *IEEE Trans. Microw. Theory Techn.*, vol. 64, no. 8, pp. 2596–2604, Aug. 2016.

[15] M. Bona, L. Manholm, J. P. Starski, and B. Svensson, "Low-loss compact Butler matrix for a microstrip antenna," *IEEE Trans. Microw. Theory Techn.*, vol. 50, no. 9, pp. 2069–2075, Sep. 2002.

[16] Y.-Z. Zhang, W.-L. Chio, W.-Y. Zhuang, W.-W. Choi, and K.-W. Tam, "Size reduction of microstrip crossover using defected ground structure and its application in Butler matrix," in *Proc. IEEE Int. Workshop Electromagn., Appl. Student Innov. Competition*, Kowloon, China, Aug. 2013, pp. 100–103.

[17] Y. J. Cheng, X. Y. Bao, and Y. X. Guo, "60-GHz LTCC miniaturized substrate integrated multibeam array antenna with multiple polarizations," *IEEE Trans. Antennas Propag.*, vol. 61, no. 12, pp. 5958–5967, Dec. 2013.

[18] T. M. Macnamara, "Positions and magnitudes of fixed phase shifters in Butler matrices incorporating 90 degrees hybrids," *IEE Proc. H Microw., Antennas Propag.*, vol. 135, no. 5, pp. 359–360, Oct. 1988.
[19] C. D. Nantista and S. G. Tantawi, "A compact, planar, eight-port waveguide power divider/combiner: The cross potent superhybrid," *IEEE Microw. Guided Wave Lett.*, vol. 10, no. 12, pp. 520–522, Dec. 2000.
[20] Y. J. Cheng, W. Hong, and K. Wu, "Millimeter-wave multibeam antenna based on eight-port hybrid," *IEEE Microw. Wireless Compon. Lett.*, vol. 19, no. 4, pp. 212–214, Apr. 2009.
[21] G. P. Riblet, "Compact planar microstrip-slotline symmetrical ring eight-port comparator circuits," *IEEE Trans. Microw. Theory Techn.*, vol. 38, no. 10, pp. 1421–1426, Oct. 1990.
[22] B. Mayer and R. Knoechel, "Novel branchline couplers for monolithic microwave integrated circuits," in *Proc. 20th Eur. Microw. Conf.*, Budapest, Hungary, 1990, pp. 1157–1162.
[23] D. M. Pozar, *Microwave Engineering*, 4th ed. New York, NY, USA: Wiley, 2012, pp. 343–347.
[24] B. W. Xu, S. Y. Zheng, Y. M. Pan, and Y. H. Huang, "A universal reference line-based differential phase shifter structure with simple design formulas," *IEEE Trans. Compon., Packag., Manuf. Technol.*, vol. 7, no. 1, pp. 123–130, Jan. 2017.
[25] Y. Wang, A. M. Abbosh, and B. Henin, "Broadband microwave crossover using combination of ring resonator and circular microstrip patch," *IEEE Trans. Compon., Packag., Manuf. Technol.*, vol. 3, no. 10, pp. 1771–1777, Oct. 2013.
[26] R. A. De Lillo, "A high performance 8-input, 8-output Butler matrix beamforming network for ultra-broadband applications," in *Proc. IEEE Antennas Propag. Soc. Int. Symp.*, Ann Arbor, MI, USA, vol. 1, Jun./Jul. 1993, pp. 474–477.
[27] T.-Y. Chin, J.-C. Wu, S.-F. Chang, and C.-C. Chang, "A V-band 8×8 CMOS Butler matrix MMIC," *IEEE Trans. Microw. Theory Techn.*, vol. 58, no. 12, pp. 3538–3546, Dec. 2010.
[28] I. Slomian, K. Wincza, K. Staszek, and S. Gruszczynski, "Folded single-layer 8×8 Butler matrix," *J. Electromagn. Waves*, vol. 31, no. 14, pp. 1386–1398, 2017.
[29] R. J. Mailloux, *Phased Array Antenna Handbook*, 2nd ed. Boston, MA, USA: Artech House, 2005.

QINGLING YANG received the M.S. degree from the University of Electronic Science and Technology of China (UESTC), Chengdu, China, in 2017. He is currently pursuing the Ph.D. degree with the University of Kent, Canterbury, Kent, U.K. His research interests include millimeter-wave antennas, multibeam antennas, and phased array antennas.

STEVEN GAO (M'01–SM'16–F'19) received the Ph.D. degree from Shanghai University, Shanghai, China.

He is currently a Professor and the Chair of RF and Microwave Engineering, and the Director of Postgraduate Research with the School of Engineering and Digital Arts, University of Kent, Canterbury, U.K. He has coedited or coauthored three books, including *Space Antenna Handbook* (Wiley, 2012), *Circularly Polarized Antennas* (Wiley-IEEE, 2014), *Low-Cost Smart Antennas* (Wiley, 2019), and more than 300 articles. He holds eight patents. His current research interests include smart antenna, phased array, multi-in multi-out (MIMO), broadband and multiband antennas, small antennas, RF front ends, FSS, and their applications into 5G mobile communications, satellite communication, small satellites, radars, energy harvesting, and medical systems.

Dr. Gao is a Fellow of the Royal Aeronautical Society and the IET. He received the 2016 IET Premium Award for the Best Paper in *IET Microwave, Antennas and Propagation* and the 2017 CST University Publication Award for a article in the IEEE TRANSACTIONS ON ANTENNAS AND PROPAGATION. He was the General Chair of the 2013 Loughborough Antenna and Propagation Conference. He is an Associate Editor of several journals, including the IEEE TRANSACTIONS ON ANTENNAS AND PROPAGATION, *Radio Science*, *Electronics Letters*, IEEE ACCESS, and *IET Circuits, Devices and Systems*, the Editor-in-Chief of Wiley Book *Series on Microwave and Wireless Technologies*, an Editorial Board Member of many international journals, the Guest Editor of PROCEEDINGS OF THE IEEE for Special Issue on Small Satellites, in 2018, the Guest Editor of the IEEE TRANSACTIONS ON ANTENNAS AND PROPAGATION for Special Issue on Antennas for Satellite Communication, in 2015, and the Guest Editor of *IET Circuits, Devices and Systems* for Special Issue in Photonic and RF Communications Systems, in 2014. He was a Distinguished Lecturer of the IEEE Antennas and Propagation Society. He was an invited speaker in many international conferences.

QI LUO (S'08–M'12–SM'19) was born in Chengdu, China, in 1982. He received the M.Sc. degree (Hons.) from the University of Sheffield, Sheffield, U.K., in 2006 and the Ph.D. degree (Hons.) from the University of Porto, Porto, Portugal, in 2012.

From 2012 to 2013, he was with the Surrey Space Centre, Guildford, U.K., as a Research Fellow. He is currently with the School of Engineering and Digital Arts, University of Kent, Canterbury, U.K., as a Research Fellow. He has authored or coauthored two books *Circularly Polarized Antennas* (Wiley-IEEE, 2014) and *Low-Cost Smart Antennas* (Wiley, 2019). He also authored a book chapter in *Handbook of Antenna Technologies* (Singapore: Springer, 2014). His current research interests include smart antennas, circularly polarized antennas, reflectarray, transmitarray, multiband microstrip antennas, and electrically small antenna design.

Dr. Luo has been serving as a reviewer for a number of technical journals and international conferences. He was awarded as the Outstanding Reviewers of the IEEE TRANSACTIONS ON ANTENNAS AND PROPAGATION, in 2015.

LEHU WEN received the M.S. degree from Xidian University, Xi'an, China, in 2011. He is currently pursuing the Ph.D. degree with the University of Kent, Canterbury, Kent, U.K. His current research interests include base station antennas, mobile terminal antennas, and tightly coupled array antennas.

XIAOFEI REN is currently with the China Research Institute of Radiowave Propagation, Xinxiang, Henan, China.

JIAN WU is currently with the China Research Institute of Radiowave Propagation, Xinxiang, Henan, China.

YONG-LING BAN was born in Henan, China. He received the B.S. degree in mathematics from Shandong University, in 2000, the M.S. degree in electromagnetics from Peking University, in 2003, and the Ph.D. degree in microwave engineering from the University of Electronic Science and Technology of China (UESTC), in 2006. In July 2006, he joined the Xi'an Mechanical and Electric Information Institute as a Microwave Engineer. He then joined Huawei Technologies Company, Ltd., Shenzhen, China. At Huawei, he designed and implemented various terminal antennas for 15 data card and mobile phone products customized from leading telecommunication industries, such as Vodafone. From September 2010 to July 2016, he was an Associate Professor with UESTC. From May 2014 to April 2015, he visited Queen Mary University of London as a Scholar Visitor. He is currently a Professor with UESTC. He is the author of over 110 refereed journal and conference papers on these topics. He holds 20 granted and pending chinese and overseas patents. His research interests include wideband small antennas for 4G/5G handset devices, MIMO antenna, and millimeter wave antenna array.

XUEXIA YANG (M'05–SM'17) received the B.S. and M.S. degrees from Lanzhou University, Lanzhou, China, in 1991 and 1994, respectively, and the Ph.D. degree in electromagnetic field and microwave technology from Shanghai University, Shanghai, China, in 2001. From 1994 to 1998, she was a Teaching Assistant and a Lecturer with Lanzhou University. From 2001 to 2008, she was a Lecturer and an Associate Professor with Shanghai University. She is currently a Professor and the Head of the Antennas and Microwave R&D Center, Shanghai University. She has authored or coauthored more than 180 technical journal and conference papers. She is also a frequent reviewer for more than ten scientific journals. Her current research interests include antennas theory and technology, computational electromagnetic, and microwave power transmission. Dr. Yang is a member of the Committee of Antenna Society of China Electronics Institute and the Senior Member of China Electronics Institute. She is an Associate Editor of the *Journal of Shanghai University* (Science Edition).